Indian Pacing and Electrophysiology Journal 22 (2022) 225–230

Contents lists available at ScienceDirect

Indian Pacing and Electrophysiology Journal

journal homepage: www.elsevier.com/locate/IPEJ

CMR - Late gadolinium enhancement characteristics associated with monomorphic ventricular arrhythmia in patients with non-ischemic cardiomyopathy

Priyanka Rajinthan [a], Kevin Gardey [a], Sara Boccalini [b], Salim Si-Mohammed [b, d], Arnaud Dulac [a], Clothilde Berger [a], Leslie Placide [a], Antoine Delinière [a], Nathan Mewton [e], Philippe Chevalier [a], Francis Bessière [a, c, *]

[a] Cardiac Electrophysiology Department, Hôpital Cardiologique Louis Pradel, 28 Avenue du Doyen Lépine, 69394, Lyon Cedex 03, Hospices Civils de Lyon, France
[b] Radiology Department, Hôpital Cardiologique Louis Pradel, 28 Avenue Du Doyen Lépine, 69394 LYON Cedex 03, Hospices Civils de Lyon, France
[c] LabTau, INSERM U 1032, Université Claude Bernard Lyon 1, France
[d] Creatis, UMR CNRS 5220, INSERM U 1044, Université Claude Bernard Lyon 1, France
[e] Centre d'investigation Clinique, Hôpital Cardiologique Louis Pradel, 28 Avenue Du Doyen Lépine, 69394, Lyon Cedex 03, Hospices Civils de Lyon, France

ARTICLE INFO

Article history:
Received 21 March 2022
Received in revised form
27 June 2022
Accepted 22 July 2022
Available online 2 August 2022

1. Introduction

Sudden cardiac death accounts for a third of overall death in non-ischemic cardiomyopathy (NICM) [1]. Predicting sudden cardiac death is a major challenge in the care of NICM and has currently mostly been based on impaired left ventricular ejection fraction (LVEF) cut-off value below 35% to decide whether to implant a defibrillator. The most recent American and European guidelines highlight the potential benefit of cardiac magnetic resonance (CMR) for sudden cardiac death risk stratification [2]. Late gadolinium enhancement (LGE) is observed in about 40% of patients with NICM [3,4]. The presence of scar and myocardial tissue heterogeneity as depicted by LGE with good levels of reproducibility has been linked to ventricular arrhythmias in ischemic, hypertrophic, and dilated cardiomyopathies [5]. It highlights the presence of myocardial fibrosis as a potential source of macro re-entries. Scar tissue depicted by LGE can be divided in two components: the core (dense scar which does not conduct) and a border zone (BZ; heterogeneous scar area which can conduct but with a slower propagation compared to healthy tissue). Corridors (described as conducting channels, CC), inside the BZ area can connect viable tissue to healthy myocardium and thus create a path for re-entrant circuit leading to VT [6,7]. LGE-CMR 3D reconstruction is now able to define the scar and CC and is already used to guide complex ventricular tachycardia (VT) ablation procedures. Correlations of border zone and scar core between voltage mapping and LGE-CMR 3D reconstructions have been reported in observational studies [8]. While LGE-CMR 3D reconstructions provide useful anatomical information to perform safest and more efficient catheter ablation procedure, they may be helpful in NICM to detect the pro-arrhythmic characteristics of a given scar. In the present study we aimed to assess whether the presence of CC is associated with ventricular arrhythmia in NICM patients with positive LGE.

2. Methods

2.1. Study oversight

A retrospective single-center case-control study was performed in a tertiary referral university hospital (Hôpital cardiologique Louis

* Corresponding author. Hôpital cardiologique Louis Pradel, Département de rythmologie et de stimulation cardiaque, Hospices Civils de Lyon, France.
E-mail address: francis.bessiere@chu-lyon.fr (F. Bessière).
Peer review under responsibility of Indian Heart Rhythm Society.

https://doi.org/10.1016/j.ipej.2022.07.007

Pradel, Hospices Civils de Lyon, France). The study was approved by the appropriate institutional review boards (NCT04607265). Written informed consent was obtained in all patients.

2.2. Patients

Consecutive NICM patients admitted for a VT ablation with a pre-operative cardiac-CMR that demonstrated a scar were enrolled (case group) for a period of two years.

Within the same study period, NICM patients without ventricular arrhythmia but with a scar (i.e. presence of LGE) on CMR were selected from the radiology department database and matched (ratio 2:1) to cases. The matching was based on the age of the patients, the mean LVEF, the cardiomyopathy's etiology; the time between the initial diagnosis and the CMR examination.

Patients whose CMR was affected by device-related artefacts that jeopardize LGE interpretation were excluded. Diagnosis of non-ischemic cardiomyopathy was based on medical history, clinical presentation and CMR findings. DCM was defined using international society and federation of cardiology definition as the presence of an elevated LV end diastolic volume indexed to body surface and systolic dysfunction. Post-myocarditis cardiomyopathy was defined as the persistence of a myocardial scar in MRI (i.e. persistence of LGE) more than 6 months after the acute myocarditis and with no oedema described in the MRI [9]. Were excluded patient presenting with a coronary artery disease (define as coronary stenosis with more than 50%) [14]; evidence of acute myocarditis; ongoing inflammatory myocardial disease; hypertrophic cardiomyopathy; arrhythmogenic right ventricular cardiomyopathy and significant valve disease. Baseline characteristics including age, gender LVEF, medication, rate of ICD implants were recorded.

3. CMR acquisition protocol

Cardiac magnetic resonance imaging was performed using a 1.5 T CMR system (Philips Ingenia, Best, the Netherland; or Siemens Avanto, Erlangen, Germany). Cine-steady state free precession sequences in the 4-chamber view, RV outflow tract and short axis view covering the entire volume of the left ventricle were performed. LGE images were obtained more than 10 min after gadolinium injection using a 3D inversion-recovery (IR) gradient echo sequence. The heart was imaged in 1 or 2 breath-holds with a spatial resolution of 2,11x1,56 × 5 mm or 1,78x2,05 × 8 mm depending on the CMR system used (Supplementary data Annex 1).

3.1. CMR analysis

Presence and location of LGE was determined by two senior operators. In case of discrepancy, a third operator settled the decision.

CMR images were then exported in DICOM format and analyzed using software designed for scar segmentation (ADAS 3D; Galgo Medical, Barcelona, Spain; Fig. 1 & 2). Delineation of endocardial and epicardial borders was done semi-automatically on the stack of short axis images using an atlas-based segmentation technique initialized with 4 anatomic landmarks (left ventricular apex, mitral ring, aortic ring, and tricuspid ring). A manual correction was required afterwards. The left ventricle was segmented in to 9 concentric layers from endocardium to epicardium: 10%, 20%, 30%, 40%, 50%, 60%, 70%, 80% and 90%, respectively, of wall thickness. Pixel signal intensity (SI) maps were obtained for each layer and color-coded to visualize its distribution [10]. Scar core and BZ were defined using an algorithm based on maximal pixel intensity (MPI) in the left ventricle. Previous studies that compared SI maps to electro-anatomical mapping (EAM) maps showed that thresholds to define scar core and BZ are respectively >60% and 40–60% of maximal SI [11]. Thus, thresholds were calculated between scar core and BZ as 60% of maximum pixel intensity (MPI) and between border zone and healthy tissue as 40% of MPI. Distribution of scar core and BZ were visualized in 3D color-coded map. CC were defined automatically as a viable myocardial path within the BZ surrounded by scar core/mitral annulus (serving as electrical isolation) and connecting healthy tissue. To qualify as a CC, the length of the path had to be above a pre-specified threshold. Scar and CC mass were obtained by multiplying the product of all the voxels for each region by the myocardial density of 1.05 g. CMR 3D reconstruction images were analyzed by two independents readers (PR, SB) blinded to the clinical and electrophysiology data, on a dedicated workstation. A third independent reader, an experienced radiologist (SS) also blinded to the medical history, was asked to analyze and assess the presence or not of CC in case of disagreement.

3.2. Electro anatomical mapping analysis

Left ventricular EAM (CARTO 3; Biosense Webster, CA, USA) was performed in order to identify the endocardial and/or epicardial voltage map during sinus or right ventricular pacing during VT catheter ablation procedure in case group. Access to the left ventricle was achieved using a retrograde, transseptal or epicardial approach. Ventricular mapping was performed using a multipolar mapping catheter (Pentharay; Biosense Webster, CA, USA). The peak-to-peak signal amplitude of the bipolar electrogram was set between 0.5 and 1.5 mV. Isthmuses of targeted VT were localized by activation and entrainment mapping if VT was hemodynamically tolerated or by pace mapping and correlation analysis if VT was not sustained or poorly tolerated. Radiofrequency was delivered to the location considered to be part of the VT isthmuses. Locations of the ablated site were then compared side-by-side to the CC obtained from the LGE-CMR 3D reconstruction. Two senior electrophysiologists (FB, KG) were asked to determine the matching between ablated sites and CMR-reconstruction. In case of discrepancy, a third electrophysiologist assessed the agreement (PC).

3.3. Statistical analysis

Differences between cases and controls regarding continuous variables were reported as mean ± SD and significance of the associations assessed using Wilcoxon rank sum test. Discrete variables were reported as proportions (percentage) and compared using Fisher's exact test. The association between CC and VT, was assessed using a Fisher Test to test the association between the two variables. Inter-observer agreement for discrete variables was assessed using Cohens Kappa coefficient. Inter-observer agreement for continuous variable was evaluated using Pearson's correlation coefficient. A two-tailed Fisher test with a 5% alpha risk was performed for the main analysis (association between VT and presence of conducting channels). Statistical analyses were performed using R version 3.6.3 (R Foundation for Statistical Computing, Vienna, Austria).

4. Results

4.1. Clinical characteristics

Between January 2017 and December 2019, 110 patients underwent VT ablation in our institution, 50 (45.5%) of whom had CMR prior to the ablation. Among the latter, 11(22%) had a non-ischemic cardiomyopathy. One patient whose CMR had defibrillator-related artefacts was excluded. Thus, a total of 10

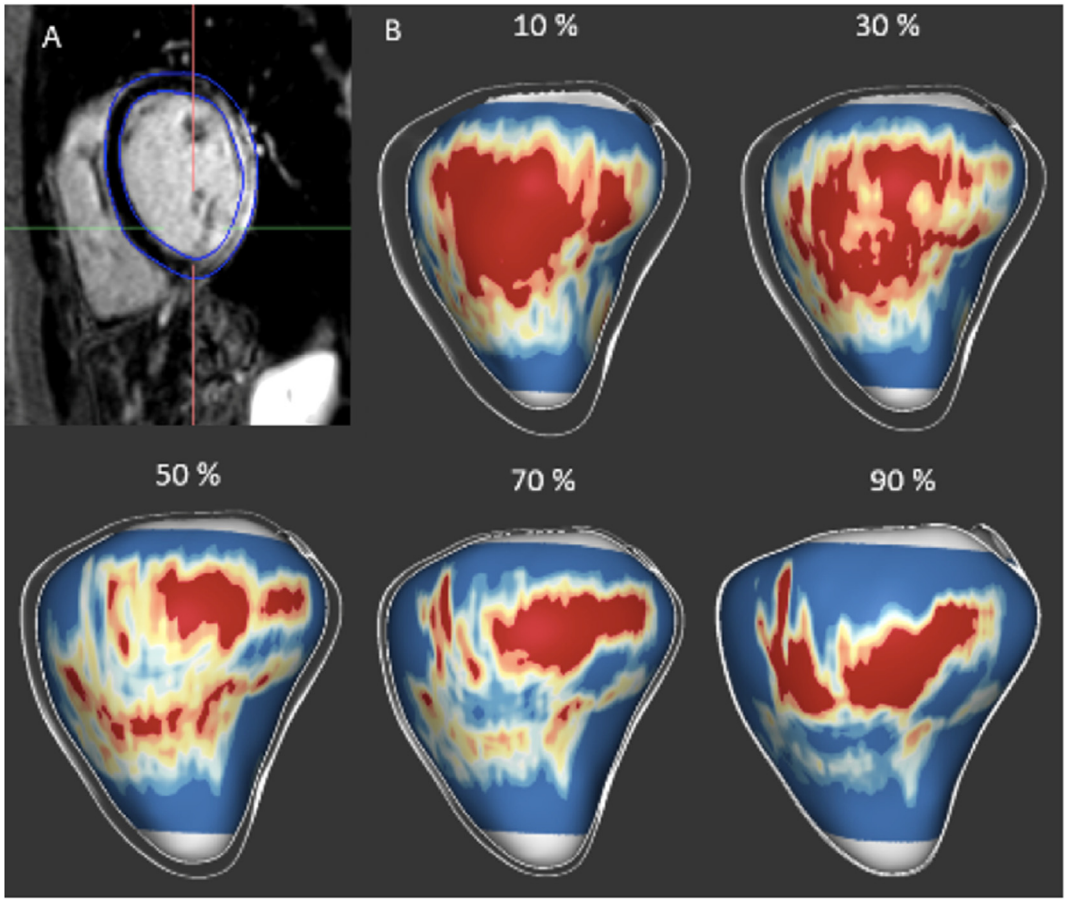

Fig. 1. Image processing of CMR analysis. A. short-axis view of endocardium and epicardium delineation; B. View of the left ventricle reconstruction from endocardium to epicardium with a color-coded pixel signal intensity map. Healthy myocardium is in blue; core is in red and border zone is in yellow and orange (scar = red + orange + yellow).

patients were included in the VT group. All patient presented monomorphic VT, 6 of them were hemodynamically well tolerated. These were matched to 20 patients with NICM and myocardial fibrosis but no history of VT (control group).

There was no significant difference between groups in terms of mean ± SD age (54.0 ± 16 versus 54.6 ± 16 years, p = 0.43), LVEF (46 ± 11.9 versus 49 ± 12.4%, p = 0.37), left ventricular end-diastolic volume (LVEDV; 88 ± 21.3 versus 95.9 ± 20 ml, p = 0.34), and the interval between initial diagnosis and CMR (12.5 ± 7.3 versus 15.7 ± 17.3 months, p = 0.65; Table 1). One patient in the VT group, and 2 in the control group had a LVEF <35%. Distribution of dilated cardiomyopathy and post-myocarditis cardiomyopathy was the same in both groups (respectively 70% and 30%).

4.2. LGE characteristics

There was no difference regarding LGE distribution between the two groups. LGE was mostly located in the free-wall (respectively 90% in the case group and 75% in the control group) and was mostly sub-epicardial (respectively 50% and 55%). All data are provided in Table 2.

4.3. Core and border zone of the scar

Although the trend was no significant, scar components were greater in the VT group than in the control group: total scar mass: 26.2 ± 27.3 g versus 13.9 ± 9.2 g, p = 0.2; core mass: 6.9 ± 6.1 g versus 3.2 ± 2.3 g, p = 0.1; BZ mass: 19.4 ± 21.6 versus 10.7 ± 7.7 g, p = 0.3. One subject in VT group had an extreme value for these parameters which explained the high standard deviation in this group. Similarly, scar mass ratio expressed as a proportion of total LV mass was also greater in the VT group (mean ± SD: 29 ± 31.8% versus 17.3 ± 14.2%; p = 0.3). Interestingly, the scar heterogeneity (assessed through the proportion of the scar that is BZ) seems comparable in the 2 groups (70.4 ± 14.1 versus 74 ± 17.4; p = 0.6; Table 3).

4.4. Conducting channels

Scars characteristics from patients with VT were significantly different than those in the control group. n = 10 (100%) VT patients had conducting channels versus 5 (25%) in the control group (p = 0.0002). In total, 19 conducting channels were described in the VT group (median: 1,5(IQR: 1 to 2)) and 16 in the control group (median: 0(IQR: 0 to 1)). Conducting channel mass was not significantly different between groups (4.0 ± 5.9 g in the VT group and 0.6 ± 1.5 g in the control group (p = 0.29). The number of conducting channels per patient was greater in the VT group (2.5 ± 1.8) than in the control group (0.8 ± 1.4; p < 0.001).

Conducting channels distribution was as follows: 46% of all the conducting channels were located in the epicardium (i.e. epicardial layer with a transmural extent ≤50%), 16% were located in the endocardium (i.e. endocardial layer with a mean transmural extent ≤50%), 5% were transmural (i.e. endocardial layer with a transmural extent >50%), and 33% were mid-myocardial (i.e. mid-myocardial distribution with an epicardial or endocardial extend < to 50% of

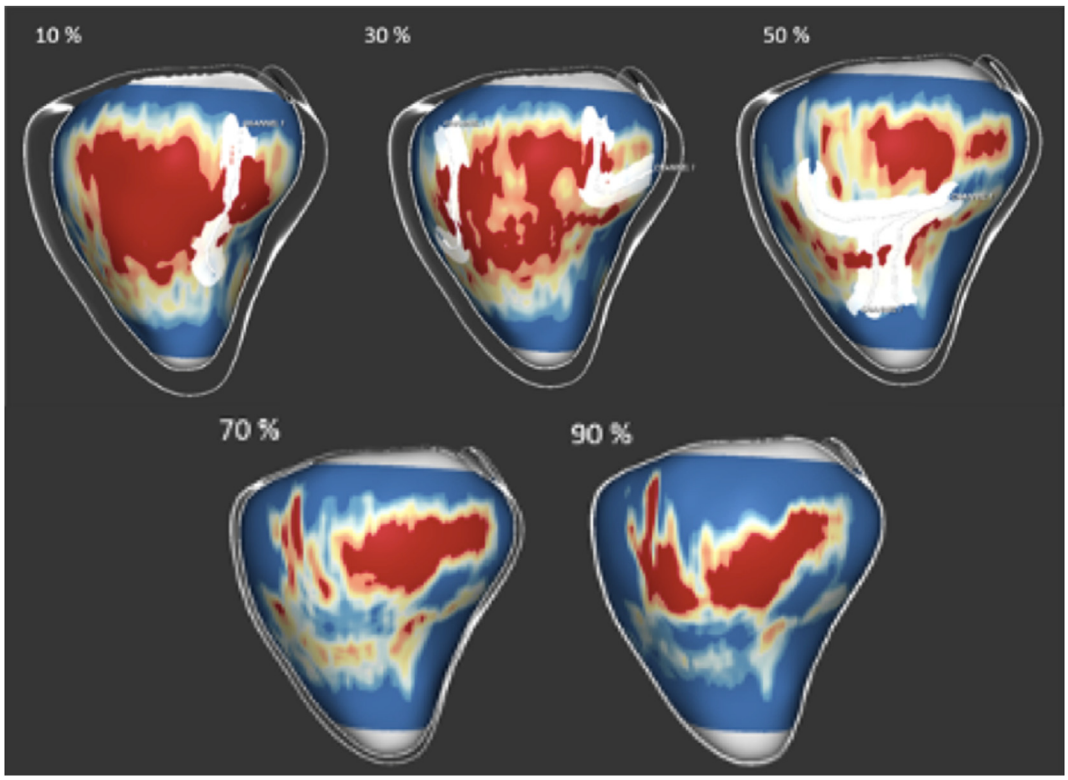

Fig. 2. Conducting channels detected by CMR reconstruction. View of the left ventricle reconstruction from endocardium to epicardium. CC are mainly located on the endocardium and mid myocardium in this example.

Table 1
Baseline characteristics.

Variable	VT group n = 10	Control group n = 20	*P*-value
Mean age, years (SD)	54 (16)	54.6 (16)	0.43
Sex (n, %)			
Men	9 (90)	18 (90)	1
Woman	1 (10)	2 (10)	1
Mean LVEF, % (SD)	46 (11.9)	49 (12.4)	0.37
Mean LVEDV; ml (SD)	88 (21.3)	95.9 (20)	0.34
DCM (n, %)	3 (30)	6 (30)	1
Post-myocarditis cardiomyopathy (n, %)	7 (70)	15 (70)	1
Mean Time from diagnosis to CMR; months (SD)	12.5 (7.3)	15.7 (17.3)	0.65
Medication			
Amiodarone (n, %)	1 (10)	0	0.33
B-blockers (n, %)	7 (70)	14 (70)	1
ACE inhibitors/Neprilysin inhibitors (n, %)	8 (80)	12 (60)	0.49
Diuretics (n, %)	0	5 (20)	0.22
ICD			
Primary prevention (n, %)	0	2 (10)	0.54
Secondary prevention (n, %)	10 (100)	0	<0.001

LVEF, left ventricular ejection fraction; LVEDV, left ventricular end diastolic volume; DCM, dilated cardiomyopathy; CMR, cardiac magnetic resonance; ACE, angiotensin-converting-enzyme inhibitors; ICE, implantable cardioverter-defibrillator.

Table 2
LGE characteristics.

	VT group	Control group	*P*-value
Septal only n,%	1 (10)	1 (5)	1
Free wall only n,%	9 (90)	15 (75)	0.6
Both n,%	0	4 (20)	0.3
Sub-epicardial only n,%	5 (50)	11 (55)	1
Mid-wall only n,%	2 (20)	3 (15)	1
Focal n,%	7 (70)	14 (70)	1
Multiple n,%	3 (30)	6 (30)	1

Table 3
CMR Scar characteristics.

	VT group n = 10	Control group n = 20	*P*-value
Mean scar mass, g	26.2 ± 27.3	13.9 ± 9.2	0.2
Mean core mass, g	6.9 ± 6.1	3.2 ± 2.3	0.1
Mean BZ mass, g	19.4 (21.6)	10.7 ± 7.7	0.3
BZ percentage of the scar	70.4 ± 14.1	74 ± 17.4	0.6
Scar percentage of LV	29 ± 31.8	17.3 ± 14.2	0.3

Values are mean ± SD; CMR = contrast-enhanced cardiac magnetic resonance; BZ = border zone; VT = ventricular tachycardia.

wall thickness).

4.5. Electro Anatomical Mapping

Electro Anatomical Mapping (EAM) access was done endo and epicardially for 7 patients and endocardially for 3 patients. Activation and/or entrainment mapping were possible in 7 patients; at each time, critical isthmus was targeted during ablation. VT were finally successfully treated in 8 patients (no recurrence after a 22 ± 6 months of follow-up). In 8 patients, 1 conducting channel described in CMR matched with ablated sites in terms of myocardial segment and layer (percentage of agreement: 80%). Among these patients: 5 were epicardial and 3 endocardial. An example is shown in Fig. 3. In one patient, EAM and CC matched the myocardial segment, but CC was described in the endocardium while the successful ablation site was done epicardially. In the other patient, both EAM and CC pointed the good layer (epicardium), but critical conducting channel was found in a slightly different segment (the infero-septal region while ablation was performed in the infero-lateral region).

5. Discussion

The present study suggests that CC may be a relevant predictive factor for monomorphic VT in NICM. CC, identified using LGE-CMR 3D segmentation, were more frequent in our NICM patients with VT compared than those with fibrosis but without VT history. In this specific patient population, CC may indicate an increased SCD risk and improve its prediction in addition to myocardial fibrosis extent alone.

To the best of our knowledge, our study is the first to investigate with a software traditionally used to guide VT ablation procedure the association between CC and occurrence of monomorphic VT in NICM. Even though the patient population is small, an association between conducting channels and VT seems likely.

Although controversial, several studies reported a correlation between scar mass as well as BZ mass and ventricular arrhythmia [12](7,13). Herein, scar mass and BZ mass were higher in the VT-group but only conducting channels were significantly more frequent in those with VT. These finding might be related to a lack of statistical power but underlines the fact that, rather than the size of the scar, it is its architecture that may contribute more to re-entrant ventricular arrhythmia. Acosta et al. found scar mass >10 g and BZ mass >5.3 g to be predictive of ventricular arrhythmia in CRT-D [14]. In the present study, scar and BZ mass in VT-group were indeed higher than these cut-off values but this was not discriminative as it was also higher in the control-group. In the other hand, Di Marco et al. didn't find any significant relation between LGE extent and VA [4]. This involves, as it was also suggested in the study reported by Acosta et al. [14], that quantitative criteria might not be sufficient to predict VT and that the detection of CC might play a key role in this risk stratification.

Recent studies also highlighted the role of LGE localization for VT prediction. The association of septal and mid-wall localization could increase the risk of SCD as demonstrated in Halliday and Al [15]. In our study, there was no difference concerning LGE localization between group although none of the patient in VT group had both localizations.

There was no difference herein regarding scar heterogeneity between the study groups. The studies that have already analyzed this parameter found an association between scar heterogeneity and occurrence of VT [13], [16]. However, the populations were different, as it was mostly patient with ischemic cardiomyopathy, while scar types and structures differ depending on the origin of cardiomyopathy [17].

5.1. Limitations

As our study has some limits, a prospective investigation with a higher number of patients with NICM is needed to establish the specific predictive value of conducting channels for gauging ventricular electrical instability in addition to myocardial fibrosis itself.

Our study principal limit is the limited number of patients included. Moreover, we included only patient with monomorphic VT and with DCM or post-myocarditis cardiomyopathy. Hence, our results could not be extrapolated to polymorphic VT or to another cardiomyopathy as HCM.

The accessibility to CMR is a potential bias. Out of the 110 patients referred for VT ablation, only 50 had a CMR prior to the intervention. CMR quality is another limit. As there was no pre-established protocol to realize acquisitions, CMR acquisition techniques were slightly different. Image quality and resolution depend

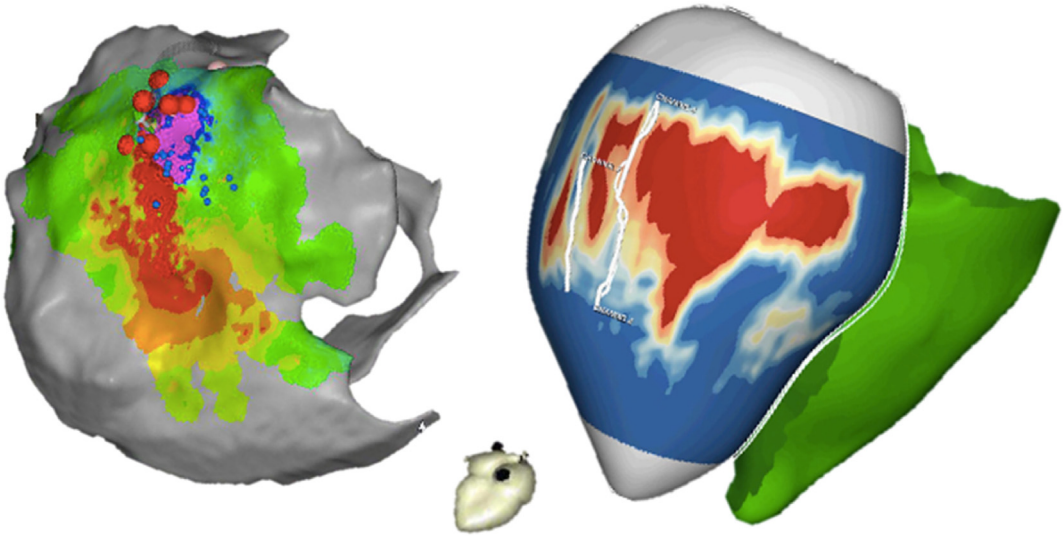

Fig. 3. Comparison of 3D activation map showing critical isthmus of an epicardial VT with its 3D- CMR analysis. The critical isthmus location matches with an epicardial conducting channel zone at the CMR.

on the length of apneas, presence of ventricular arrhythmia during acquisition, partial volume effect. 3D reconstructions may be jeopardized by artefacts and slice size. As each slice was 4–5 mm apart, some CC might not have been detected. In dense scar, the accurate delineation of endocardium and epicardium layers can be limited, generating potential errors in conducting channels display. Despite these limits, the agreement was good between LGE-CMR 3D reconstruction and EAM.

Interestingly, and in opposition to most of the studies conducted until now, a large majority of patients included in our cohort had an LVEF ≥35%. From now, arrhythmic risk stratification was mainly based on LVEF with a cut off value of 35%. However, LVEF remains a poorly specific and sensitive marker for SCD as recent data showed [4,18]. This highlights the need of new parameters to improve the risk stratification process. Hence, in recent years, finding a new algorithm to identify patients with a higher arrhythmogenic risk have become a major concern. In the most recent study on NICM patient, Di Marco et al. proposed a new algorithm combining LGE and LVEF [4] based on a retrospective study on 1165 patients with NICM. This algorithm shows promising results allowing the reclassification of 34% of the patient in the cohort. In line with this, our study adds a new parameter which may be interesting in this complex decision-making process: the identification of conduction channels and their characteristics.

Nonetheless, since fibrosis is an active process that gradually change over time, risk stratification needs iterative evaluation with time intervals that must be defined. Herein, the interval of time that separated initial diagnosis and CMR was the same in both groups [19]. Conducting channels may predict occurrence of monomorphic VT but much less polymorphic VT nor ventricular fibrillation [20]. While non-ischemic cardiomyopathy is a diverse group of heart diseases with variable arrhythmia substrates, non-reentrant mechanism, can also be present in patients with monomorphic VT, in the absence of slow conduction. The occurrence of monomorphic VT is then lower in NICM than in ischemic cardiomyopathy [21]. Thus, presence of conducting channels will probably not be enough to predict all ventricular events, but could be a part of the decision-making process, especially in patient with an LVEF >35% with fibrosis, who are yet not candidate for prophylactic ICD implantation.

6. Conclusion

In the present retrospective cohort study, the properties of myocardial scars differed between NICM patients who experienced or not VT. The data suggests that the presence of CC may help in establishing accurate risk factors that would predict ventricular arrhythmia, beyond myocardial mechanical dysfunction and fibrosis extent.

Clinical trial

NCT04607265.

Declaration of competing interest

None of the authors have any conflict of interest.

Acknowledgments

The authors would like to thank Dr Robinson (DRCI, Hospices Civils de Lyon) for his constructive criticism of the manuscript.

References

[1] Kadish A, Dyer A, Daubert JP, Quigg R, Estes NAM, Anderson KP, et al. Prophylactic defibrillator implantation in patients with nonischemic dilated cardiomyopathy. N Engl J Med 2004 May 20;350(21):2151–8.
[2] Priori SG, Blomström-Lundqvist C, Mazzanti A, Blom N, Borggrefe M, Camm J, et al. 2015 ESC guidelines for the management of patients with ventricular arrhythmias and the prevention of sudden cardiac death: the task force for the management of patients with ventricular arrhythmias and the prevention of sudden cardiac death of the European society of cardiology (ESC). Endorsed by: association for European paediatric and congenital cardiology (AEPC). Eur Heart J 2015 Nov 1;36(41):2793–867.
[3] Bogun FM, Desjardins B, Good E, Gupta S, Crawford T, Oral H, et al. Delayed-enhanced magnetic resonance imaging in nonischemic cardiomyopathy: utility for identifying the ventricular arrhythmia substrate. J Am Coll Cardiol 2009 Mar 31;53(13):1138–45.
[4] Di Marco A, Brown PF, Bradley J, Nucifora G, Claver E, de Frutos F, et al. Improved risk stratification for ventricular arrhythmias and sudden death in patients with nonischemic dilated cardiomyopathy. J Am Coll Cardiol 2021 Jun;77(23):2890–905.
[5] Anagnostopoulos I, Kousta M, Kossyvakis C, Lakka E, Paraskevaidis NT, Schizas N, et al. The prognostic role of late gadolinium enhancement on cardiac magnetic resonance in patients with nonischemic cardiomyopathy and reduced ejection fraction, implanted with cardioverter defibrillators for primary prevention. A systematic review and meta-analysis. J Interv Card Electrophysiol [Internet] 2021 Jul 3 [cited 2021 Dec 1]; Available from, https://link.springer.com/10.1007/s10840-021-01027-6.
[6] Andreu D, Ortiz-Pérez JT, Fernández-Armenta J, Guiu E, Acosta J, Prat-González S, et al. 3D delayed-enhanced magnetic resonance sequences improve conducting channel delineation prior to ventricular tachycardia ablation. EPP Eur 2015 Jun;17(6):938–45.
[7] Balaban G, Halliday BP, Porter B, Bai W, Nygård S, Owen R, et al. Late-gadolinium enhancement interface area and electrophysiological simulations predict arrhythmic events in patients with nonischemic dilated cardiomyopathy. JACC Clin Electrophysiol 2021 Feb;7(2):238–49.
[8] Mukherjee RK, Whitaker J, Williams SE, Razavi R, O'Neill MD. Magnetic resonance imaging guidance for the optimization of ventricular tachycardia ablation. EPP Eur 2018 Nov 1;20(11):1721–32.
[9] Cannata' A, Artico J, Gentile P, Merlo M, Sinagra G. Myocarditis evolving in cardiomyopathy: when genetics and offending causes work together. Eur Heart J Suppl 2019 Mar 1;21(Supplement_B):B90–5.
[10] Fernández-Armenta J, Berruezo A, Andreu D, Camara O, Serra L, Barbarito V, et al. Three-dimensional architecture of scar and conducting channels based on high resolution ce-CMR: insights for ventricular tachycardia ablation. Circ Arrhythm Electrophysiol 2013 Jun;6(3):528–37.
[11] Andreu D, Berruezo A, Ortiz-Pérez JT, Silva E, Mont L, Borràs R, et al. Integration of 3D electroanatomic maps and magnetic resonance scar characterization into the navigation system to guide ventricular tachycardia ablation. Circ Arrhythm Electrophysiol 2011 Oct;4(5):674–83.
[12] Gulati A, Jabbour A, Ismail TF, Guha K, Khwaja J, Raza S, et al. Association of fibrosis with mortality and sudden cardiac death in patients with nonischemic dilated cardiomyopathy. JAMA 2013 Mar 6;309(9):896.
[13] Fernandez-Armenta J, Berruezo A, Mont L, Sitges M, Andreu D, Silva E, et al. Use of myocardial scar characterization to predict ventricular arrhythmia in cardiac resynchronization therapy. Europace 2012 Nov 1;14(11):1578–86.
[14] Acosta J, Fernández-Armenta J, Borràs R, Anguera I, Bisbal F, Martí-Almor J, et al. Scar characterization to predict life-threatening arrhythmic events and sudden cardiac death in patients with cardiac resynchronization therapy. JACC Cardiovasc Imaging 2018 Apr;11(4):561–72.
[15] Halliday BP, Baksi AJ, Gulati A, Ali A, Newsome S, Izgi C, et al. Outcome in dilated cardiomyopathy related to the extent, location, and pattern of late gadolinium enhancement. JACC Cardiovasc Imaging 2019 Aug;12(8):1645–55.
[16] Malaczynska-Rajpold K, Blaszyk K, Kociemba A, Pyda M, Posadzy-Malaczynska A, Grajek S. Islets of heterogeneous myocardium within the scar in cardiac magnetic resonance predict ventricular tachycardia after myocardial infarction. J Cardiovasc Electrophysiol 2020 Jun;31(6):1452–61.
[17] Bing R, Dweck MR. Myocardial fibrosis: why image, how to image and clinical implications. Heart 2019 Dec;105(23):1832–40.
[18] Halliday BP, Gulati A, Ali A, Guha K, Newsome S, Arzanauskaite M, et al. Association between midwall late gadolinium enhancement and sudden cardiac death in patients with dilated cardiomyopathy and mild and moderate left ventricular systolic dysfunction. Circulation 2017 May 30;135(22):2106–15.
[19] Travers JG, Kamal FA, Robbins J, Yutzey KE, Blaxall BC. Cardiac fibrosis: the fibroblast awakens. Circ Res 2016 Mar 18;118(6):1021–40.
[20] Piers SRD, Everaerts K, van der Geest RJ, Hazebroek MR, Siebelink H-M, Pison LAFG, et al. Myocardial scar predicts monomorphic ventricular tachycardia but not polymorphic ventricular tachycardia or ventricular fibrillation in nonischemic dilated cardiomyopathy. Heart Rhythm 2015 Oct;12(10):2106–14.
[21] Steinberg BA, Mulpuru SK, Fang JC, Gersh BJ. Sudden death mechanisms in nonischemic cardiomyopathies: insights gleaned from clinical implantable cardioverter-defibrillator trials. Heart Rhythm 2017 Dec;14(12):1839–48.